

Granger causality and the inverse Ising problem

Mario Pellicoro* and Sebastiano Stramaglia†

*Dipartimento Interateneo di Fisica, Università di Bari, I-70126 Bari, Italy,
TIRES-Center of Innovative Technologies for Signal Detection and Processing, Università di Bari, Italy, and
I.N.F.N., Sezione di Bari, I-70126 Bari, Italy*
(ΩDated: June 16, 2010)

The inference of the couplings of an Ising model with given means and correlations is called *inverse Ising problem*. This approach has received a lot of attention as a tool to analyze neural data. We show that autoregressive methods may be used to learn the couplings of an Ising model, also in the case of asymmetric connections and for multi-spin interactions. We find that, for each link, the linear Granger causality is two times the corresponding transfer entropy (i.e. the information flow on that link) in the weak coupling limit. For sparse connections and a low number of samples, the ℓ_1 regularized least squares method is used to detect the interacting pairs of spins. Nonlinear Granger causality is related to multi-spin interactions.

PACS numbers: 05.10.-a, 05.45.Tp, 87.18.Sn

I. INTRODUCTION

A large number of neurons is involved in any computation, and the presence of non-trivial correlations makes understanding the mechanisms of computation in brain a difficult challenge [1]. The simplest model for describing multi-neuron spike statistics is the pairwise Ising model [2, 3]. The inference of the couplings of an Ising model from data, the *inverse Ising problem*, has recently attracted attention, see [4] where data from a simulated cortical network were considered; the general idea is to find an Ising model with the same means and pairwise correlations as the data. Several approximate methods can be used, like that by Sessak and Monasson [5] or the inversion of TAP equations [6]: equal-time correlations from data are used in those methods [7]. The flow of information between spins is related, instead, to correlations at different times between variables: it can be expected that measuring the information flow between spins one may improve the estimate of couplings from data.

Two major approaches are commonly used to estimate the information flow between variables, transfer entropy [8] and Granger causality [9]. Recently it has been shown that for Gaussian variables Granger causality and transfer entropy are entirely equivalent as the following relation holds: *Granger causality* = 2 *Transfer Entropy*. This result provides a bridge between autoregressive and information-theoretic approaches to causal inference from data [10].

The purpose of this work is to explore the use of Granger causality to learn Ising models from data. The *inverse Ising problem* is here seen as belonging to the more general frame of the inference of dynamical networks from data, a topic which has been studied in recent papers [11–14]: its relevance is due to the fact that dynamical networks [15] model physical and biological behavior in many applications [16]. We show that for weak couplings, the linear Granger causality of each link is two times the corresponding transfer entropy, also for Ising models: this occurrence justifies the use of autoregressive approaches to the inverse Ising problem. In the same limit, for each link, the following relation exists between the coupling (J) and the causality (δ): $\delta = J^2$. In the case of limited samples, Granger causality gives poor results: almost all the connections are not assessed as significant for low number of samples. In these cases, we propose the use of ℓ_1 least squares method [17], a penalized autoregressive approach tailored to embody the sparsity assumption, to recover the non-vanishing connections of a sparse Ising model; as expected the ℓ_1 approach outperforms Granger causality in this case. Finally we show that nonlinear Granger causality is related to multi-spin interactions.

The paper is organized as follows. In the next section we briefly recall the notions of Granger causality and transfer entropy, and we also describe the Ising models that we use for simulations. In section III we describe our results on fully connected models, sparse Ising models and models with higher order spin interactions. Some conclusions are drawn in section IV.

*Electronic address: mario.pellicoro@ba.infn.it

†Electronic address: sebastiano.stramaglia@ba.infn.it

II. GRANGER CAUSALITY AND TRANSFER ENTROPY

In this section we review the notions of Granger causality analysis and transfer entropy. We also discuss the application of these methods to binary time series arising from Ising models.

A. Granger causality

Granger causality has become the method of choice to determine whether and how two time series exert causal influences on each other [18]. It is based on prediction: if the prediction error of the first time series is reduced by including measurements from the second one in the linear regression model, then the second time series is said to have a causal influence on the first one [19]. The estimation of linear Granger causality from Fourier and wavelet transforms of time series data has been recently addressed [20]. The nonlinear generalization of Granger causality has been developed by a kernel algorithm which embeds data into a Hilbert space, and searches for linear Granger causality in that space [21]; the embedding is performed implicitly, by specifying the inner product between pairs of points [22], and a statistical procedure is used to avoid over-fitting.

Quantitatively, let us consider n time series $\{x_\alpha(t)\}_{\alpha=1,\dots,n}$ [23]; the lagged state vectors are denoted

$$X_\alpha(t) = (x_\alpha(t-m), \dots, x_\alpha(t-1)),$$

m being the window length. Let $\epsilon(x_\alpha|\mathbf{X})$ be the mean squared error prediction of \mathbf{x}_α on the basis of all the vectors \mathbf{X} (corresponding to the kernel approach described in [21]): $\epsilon(x_\alpha|\mathbf{X})$ is equal to $1 - \tilde{\mathbf{x}}_\alpha^\top \tilde{\mathbf{x}}_\alpha$, where $\tilde{\mathbf{x}}_\alpha$, the predicted values of \mathbf{x}_α using \mathbf{X} , is the projection of \mathbf{x}_α on a suitable space H . The prediction of \mathbf{x}_α on the basis of all the variables but X_β , $\epsilon(x_\alpha|\mathbf{X} \setminus X_\beta)$, corresponds instead to the projection on a space H' with $H = H' \oplus H^\perp$. H^\perp represents the information that one gains from the knowledge of X_β . The multivariate Granger causality index $\delta(\beta \rightarrow \alpha)$ is defined as the (normalized) variation of the error in the two conditions, i.e.

$$\delta(\beta \rightarrow \alpha) = \frac{\epsilon(x_\alpha|\mathbf{X} \setminus X_\beta) - \epsilon(x_\alpha|\mathbf{X})}{\epsilon(x_\alpha|\mathbf{X} \setminus X_\beta)}. \quad (1)$$

Note that the numerator, in the equation above, coincides with the projection of \mathbf{x}_α on H^\perp : as described in [13], one may write

$$\delta(\beta \rightarrow \alpha) = \sum_{i=1}^m r_i^2, \quad (2)$$

where r_i are suitable Pearson's correlations. By summing, in equation (2), only over significative correlations, a *filtered* linear Granger causality index is obtained which measures the causality without further statistical test.

In [25] it has been shown that not all the kernels are suitable to estimate causality. Two important classes of kernels which can be used to construct nonlinear causality measures are the *inhomogeneous polynomial kernel* (whose features are all the monomials, in the input variables, up to the p -th degree; $p = 1$ corresponds to linear Granger causality) and the *Gaussian kernel*. Note that in [10] a different index of causality is adopted:

$$\Delta(\beta \rightarrow \alpha) = \log \frac{\epsilon(x_\alpha|\mathbf{X} \setminus X_\beta)}{\epsilon(x_\alpha|\mathbf{X})} = -\log[1 - \delta(\beta \rightarrow \alpha)]; \quad (3)$$

Δ and δ coincide at small δ . The choice of the window length m is usually done using the standard cross-validation scheme [24]; as in this work we know how data are generated, here we use $m = 1$.

The formalism of Granger causality is constructed under the hypothesis that time series assume continuous values x_α . In recent papers the application of Granger causality to data in the form of phases has been considered [26, 27]. Even though there is not theoretical justification in the case of binary variables, here we apply the formalism of Granger causality to n binary time series $\{\sigma_\alpha(t) = \pm 1\}_{\alpha=1,\dots,n}$, by substituting

$$x_\alpha(t) \rightarrow \sigma_\alpha(t)$$

and

$$X_\alpha(t) \rightarrow \sigma_\alpha(t-1) = \Sigma_\alpha(t);$$

in this work we justify the application of Granger causality to binary time series in terms of its relation with transfer entropy.

B. Transfer entropy

Using the same notation as in the previous subsection, the transfer entropy index $T_E(\beta \rightarrow \alpha)$ is given by [8]

$$T_E(\beta \rightarrow \alpha) = \int dx_\alpha \int d\mathbf{X} p(x_\alpha, \mathbf{X}) \log \frac{p(x_\alpha | \mathbf{X} \setminus X_\beta)}{p(x_\alpha | \mathbf{X})}, \quad (4)$$

and measures the flow of information from β to α . For Gaussian variables it has been shown [10] that causality is determined by the transfer entropy and $\Delta = 2T_E$; hence $\delta = 1 - e^{-2T_E}$ for Gaussian variables. The probabilities p 's, in (4), must be estimated from data using techniques of nonlinear time series analysis [28]. In the case of binary variables $\{\sigma_\alpha = \pm 1\}$, the number of configurations is finite and the integrals in (4) become sums over configurations; the probabilities can be estimated as frequencies in the data-set at hand. Therefore

$$T_E(\beta \rightarrow \alpha) = \sum_{\sigma_\alpha = \pm 1} \sum_{\Sigma_1 = \pm 1} \cdots \sum_{\Sigma_n = \pm 1} p(\sigma_\alpha, \Sigma) \log \frac{p(\sigma_\alpha, \Sigma \setminus \Sigma_\beta) p(\Sigma)}{p(\sigma_\alpha, \Sigma) p(\Sigma \setminus \Sigma_\beta)}, \quad (5)$$

where $p(\Sigma)$ is the fraction of times that the configuration Σ is observed in the data set, and similar definitions hold for the other probabilities. We remark that the number of configurations increases exponentially as the number of spins grows, hence the direct evaluation of (5) is feasible only for systems of small size.

C. Ising models

The binary time series analyzed in this work are generated by parallel updating of Ising variables $\{\sigma_\alpha\}_{\alpha=1,\dots,n}$:

$$p(\sigma_\alpha(t) = +1 | \Sigma(t)) = \frac{1}{1 + e^{-2h_\alpha(t)}}, \quad (6)$$

where the local fields are given by

$$h_\alpha(t) = \sum_{\beta=1}^n J_{\alpha\beta} \sigma_\beta(t-1) \quad (7)$$

with couplings $J_{\alpha\beta}$. Starting from a random initial configuration of the spin, equations (6) are iterated and, after discarding the initial transient regime, N consecutive samples of the system are stored for further analysis.

III. ANALYSIS OF ISING MODELS

A. Fully connected models

In order to generalize Granger causality to discrete variables, we consider the regression function of (6). For weak couplings the conditional expectation (which coincides with the regression function [30]) can be written

$$\langle \sigma_\alpha \rangle_{|\Sigma} = \sum_{s=\pm 1} s p(\sigma_\alpha = s | \Sigma) = \tanh(h_\alpha) \sim \sum_{\beta=1}^n J_{\alpha\beta} \Sigma_\beta, \quad (8)$$

and is a linear function of the couplings. Therefore the linear causality is $\delta(\beta \rightarrow \alpha) \sim J_{\alpha\beta}^2$ at the lowest order in J 's. Analogously, expanding eq.(5) at the lowest order, the transfer entropy reads $T_E(\beta \rightarrow \alpha) \sim J_{\alpha\beta}^2/2$. This means that, for low couplings, the value of J , for any given link, determines both the transfer entropy and the linear Granger causality for that link, and the two quantities differ only by the factor 2. The same relation, proved in the Gaussian case, holds also for Ising models at weak couplings. Being related to the transfer entropy, Granger causality thus measures the information flow for these systems, and this justifies the use of Granger causality methods for Ising systems. Synaptic couplings are directed, so $J_{\alpha\beta}$ is not in general equal to $J_{\beta\alpha}$ (the equilibrium Ising model requires symmetric couplings [29]). Therefore we consider an asymmetric system of spins with couplings $J_{\alpha\beta}$ chosen at random from a normal distribution with zero mean and standard deviation J_0 ; no self interactions are assumed ($J_{\alpha\alpha} = 0$). In figure (1) we report the plot of the numerical estimates of linear causality and transfer entropy, as a function of J ,

for several realizations of the couplings and for some values of J_0 ; the simulations confirm that for low couplings a one-one correspondence exists between causality and transfer entropy.

In figure (2) we depict, as a function of the coupling J , both the linear causality and the transfer entropy in a typical asymmetric model of six spins with $N = 100, 1000$ and 10000 samples, and $J_0 = 0.2$. In figure (3) we depict, as a function of the number of samples N , the difference between the values of transfer entropy and causality (as estimated on 10^6 samples) and their estimates based on N samples (the difference is averaged over 1000 runs of the Ising system): at low N the estimates of causalities are more reliable than those of transfer entropy. Moreover, the computational complexity of the estimation of transfer entropy is much higher than those corresponding to the evaluation of Granger causality.

Another interesting situation is all the couplings being equal to a positive quantity J (still, without self-interactions). In figure (4) we depict the Granger causality and the transfer entropy as a function of J (these quantities are the same for all the links, due to symmetry). For small values of J both quantities coincide with the values that correspond to J in the asymmetric model, and the relation $\delta/T_E = 2$ holds. On the other hand, as J increases, this relation is more and more violated. The departure of the ratio δ/T_E from 2 is connected to the emergence of feedback effects in the system, see e.g. the dependency, on J , of the auto-correlation time of the magnetization $n^{-1} \sum_{\alpha=1}^n \sigma_\alpha$ in fig.(5).

B. Sparse models

In many applications one may hypothesize that the connections among variables are sparse. The main goal, in those cases, is to infer the couplings which are not vanishing, independently of their strengths, in particular when the number of samples is low. Moreover, in the case of limited data, Granger causality gives poor results; indeed almost all connections would not be assessed as significative (for a given amount a data, only couplings stronger than a critical value can be recognized by Granger causality [21]).

A major approach to sparse signal reconstruction is the ℓ_1 regularized least squares method [17]. Although it has been developed to handle continuous variables, we will apply this method to the configurations of Ising models. For each target spin σ_α , the vector of couplings $A_{\alpha\beta}$, with $\beta = 1, \dots, n$, is sought for as the minimizer of

$$\sum_{t=1}^N \left(\sigma_\alpha(t) - \sum_{\beta} A_{\alpha\beta} \Sigma_\beta(t) \right)^2 + \lambda \|A_{\alpha\beta}\|_1, \quad (9)$$

where $\lambda > 0$ is a regularization parameter and $\|A_{\alpha\beta}\|_1 = \sum_{\beta=1}^n |A_{\alpha\beta}|$ is the ℓ_1 norm of the vector of couplings. As λ is increased, the number of vanishing couplings in the minimizers increases: λ controls the sparsity of the solution [31]. The strategy to fix the value of λ we use here is 10-fold cross-validation [24]: the original sample is randomly partitioned into 10 subsamples and, out of the 10 subsamples, a single subsample is retained as the validation data. The remaining 9 subsamples are used in (9) to determine the couplings A ; the quality of this solution is evaluated as the average number of errors on the validation data. The cross-validation process is then repeated 10 times (the folds), with each of the 10 subsamples used exactly once as the validation data, and the error on the validation data is averaged over the 10 folds. The whole procedure is then repeated as λ is varied. The optimal value of λ is chosen as the one leading to the smallest average error on the validation data.

As an example, we simulate a system made of 30 spins constituted by ten modules of three spins each. The non-vanishing couplings of the Ising model are given by:

$$\begin{aligned} J(3i-2, 3i-1) &= 0.2, \\ J(3i-1, 3i) &= 0.2, \\ J(3i, 3i-2) &= -0.2, \\ J(3i, 3i-1) &= 0.2, \end{aligned} \quad (10)$$

for $i = 1, 2, \dots, 10$. After evaluating the couplings $A_{\alpha\beta}$, using the algorithm described in [31], we calculate the sensitivity (fraction of non-vanishing connections J leading to non-vanishing couplings A) and the specificity (fraction of vanishing connections J leading to vanishing couplings A) as a function of λ . The ROC curves (as λ is varied, the ROC curve is sensitivity as a function of 1-specificity [32]) we obtain, in correspondence to three values of the number of samples N (100, 250 and 500), are depicted in fig. (6). The stars on the curves represent the points corresponding to the value of λ found by ten-fold cross validation; these points correspond to a good compromise between specificity and sensitivity. The empty symbols, instead, represent the values of sensitivity and specificity obtained using Granger causality in the three cases; the specificity by Granger causality is nearly one in all cases, while the sensitivity is strongly dependent on the number of samples and goes to zero as N decreases. To conclude this subsection, we have

shown that in the case of low number of samples and sparse connections the ℓ_1 regularized least squares method can be used to infer the connections in Ising models and outperforms Granger causality in these situations. We remark that direct evaluation of the transfer entropy in these cases is unfeasible.

C. Higher order spin interactions

The case of higher order spin interactions requires use of nonlinear Granger causality: in the presence of p -spins interactions, the kernel approach [21] with the polynomial kernel of at least $p - 1$ degree is needed. As an example, we consider a system of three spins with local fields given by:

$$\begin{aligned} h_1(t) &= J\sigma_2(t-1)\sigma_3(t-1), \\ h_2(t) &= 0.5\sigma_3(t-1), \\ h_3(t) &= 0.5\sigma_2(t-1). \end{aligned} \tag{11}$$

In figure (7) we depict the causalities $\delta(2 \rightarrow 1)$ and $\delta(2 \rightarrow 3)$, as a function of J , using the linear kernel and for the approach with the $p = 2$ polynomial kernel. Note that, due to symmetry, $\delta(3 \rightarrow 1) = \delta(2 \rightarrow 1)$ and $\delta(2 \rightarrow 3) = \delta(3 \rightarrow 2)$; all the other causalities are vanishing. The linear approach is not able to detect the three spins interaction, while using the nonlinear approach the interaction is correctly inferred. We stress that the presence of multispin interactions is connected to the presence of synergetic variables, see [33] for a discussion about the notions of redundancy and synergy in the frame of causality.

It is interesting to show the performance by transfer entropy on the same problem, see fig.(8): it correctly detects all the interactions, and the value of the transfer entropy is again very close to be half of those from nonlinear Granger causality. We stress that transfer entropy can be applied without prior assumptions about the order of the spins interactions. A major problem in the inference of dynamical networks is the selection of an appropriate model; in the case of transfer entropy this issue does not arise, although this advantage may be offset by problems associated with reliable estimation of entropies in sample.

IV. CONCLUSIONS

We have proposed the use of autoregressive methods to learn Ising models from data. Commonly, the formulation of the inverse Ising problem assumes symmetric interactions and is solved by exploiting the relations that exist, at equilibrium, between the pairwise correlations (at equal times) and the matrix of couplings. In the general case of asymmetric couplings, no equilibrium is reached and also time delayed correlations among spins should be used to infer the connections. We have shown that autoregressive approaches can solve the inverse Ising problem for weak couplings: for each link $|J_{\alpha\beta}| = \sqrt{\delta(\beta \rightarrow \alpha)}$, whilst the sign of J coincides with the sign of the linear correlation between σ_α and Σ_β . For weak couplings, Granger causality is proportional to the transfer entropy and requires less samples, than transfer entropy, to provide a reliable estimate of the information flow. For sparse connections and low number of samples, the ℓ_1 regularized least squares method is preferable to Granger causality; nonlinear Granger causality is related to multispin interactions.

The authors thank Amos Maritan and Marco Zamparo (University of Padova) for valuable discussions.

-
- [1] F. Rieke, D. Warland, R.R. de Ruyter van Steveninck, and W. Bialek, *Spikes: exploring the neural code* (MIT press, Cambridge, MA, 1997).
 - [2] E. Schneidman, M.J. Berry, R. Segev, W. Bialek, *Nature* **440**, 1007 (2006).
 - [3] J. Shlens, G.D. Field, J.L. Gauthier, M.I. Grivich, D. Petrusca, A. Sher, A.M. Litke, E.J. Chichilnisky, *J. Neurosci.* **28** 505 (2008).
 - [4] Y. Roudi, J. Tyrcha, J. Hertz, *Physical Review E* **79**, 051915 (2009).
 - [5] V. Sessak and R. Monasson, *J. Phys. A* **42**, 055001 (2009).
 - [6] H.J. Kappen and F.B. Rodriguez, *Neural Computation* **10**, 1137 (1998).
 - [7] Y. Roudi, E. Aurell and J.A. Hertz, *Front. Comput. Neurosci.* **3**, 22 (2009).
 - [8] T. Schreiber, *Phys. Rev. Lett.* **85**, 461 (2000).
 - [9] C.W.J. Granger, *Econometrica* **37**, 424 (1969).
 - [10] L. Barnett, A.B. Barrett, and A.K. Seth, *Phys. Rev. Lett.* **103**, 238701 (2009).
 - [11] D. Yu, M. Righero, L. Kocarev, *Phys.Rev.Lett.* **97**, 188701 (2006).
 - [12] D. Napoletani, T. Sauer, *Phys. Rev. E* **77**, 26103 (2008).

- [13] D. Marinazzo, M. Pellicoro and S. Stramaglia, Phys. Rev. E **77**, 056215 (2008).
- [14] D. Materassi, G. Innocenti, Physica A **388**, 3866 (2009).
- [15] A.L. Barabasi, *Linked: the new science of networks*. (Perseus Publishing, Cambridge Mass., 2002).
- [16] S. Boccaletti, V. Latora, Y. Moreno, M. Chavez and D.-U. Hwang, Phys. Rep. **424**, 175 (2006).
- [17] R. Tibshirani, J. Roy. Stat. Soc. **B 58**, 267 (1996).
- [18] K. Hlavackova-Schindler, M. Palus, M. Vejmelka, J. Bhattacharya, Physics Reports **441**, 1 (2007).
- [19] Y. Chen, G. Rangarajan, J. Feng, and M. Ding, Phys. Lett. **A 324**, 26 (2004).
- [20] M. Dhamala, G. Rangarajan, M. Ding, Phys.Rev.Lett. **100**, 18701 (2008).
- [21] D. Marinazzo, M. Pellicoro, S. Stramaglia, Phys. Rev. Lett. **100**, 144103 (2008).
- [22] J. Shawe-Taylor and N. Cristianini, *Kernel Methods For Pattern Analysis*. (Cambridge University Press, London, 2004).
- [23] After a linear transformation, we may assume all the time series to have zero mean and unit variance.
- [24] M. Stone, J. Roy. Stat. Soc. **B 36**, 111 (1974).
- [25] N. Ancona and S. Stramaglia, Neural Comput. **18**, 749 (2006).
- [26] L. Angelini, M. Pellicoro and S. Stramaglia, Phys. Lett. **A 373**, 2467 (2009).
- [27] D. Smirnov and B. Bezruchko, Phys. Rev. **E 79**, 046204 (2009).
- [28] H. Kantz, T. Schreiber, *Nonlinear time series analysis* (Cambridge University Press, Cambridge, 1997).
- [29] L.P. Kadanoff, *Statistical Physics* (World Scientific, Singapore, 2000).
- [30] A. Papoulis, *Probability, Random Variables and Stochastic Processes McGraw Hill, New York, 1965*.
- [31] S.J. Kim, K. Koh, M. Lustig, S. Boyd, D. Gorinevsky, IEEE J. Sel. Top. in Sig. Process. **1**, 606 (2007).
- [32] M.H. Zweig and G. Campbell, Clin. Chem. **39**, 561 (1993).
- [33] L. Angelini et al., Phys. Rev. **E 81**, 037201 (2010).

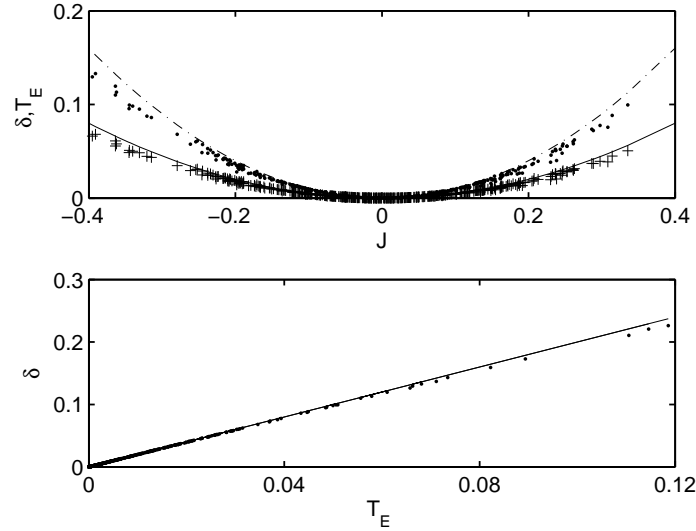


FIG. 1: (Top) The estimates of linear Granger causality and transfer entropy, for each link, are plotted versus the coupling J . The points, corresponding to 15 realizations of the couplings of six-spins Ising systems with J_0 ranging in $[0.1, 0.2]$, are displayed (the two quantities are estimated over samples of $N = 10^6$ length). The curves are the quadratic expansions at weak coupling: $\delta = J^2$ (dashed-dotted line) and $T_E = J^2/2$ (continuous line). (Bottom) The same points are displayed in the $\delta - T_E$ plane, showing that $\delta = 2T_E$ at weak coupling.

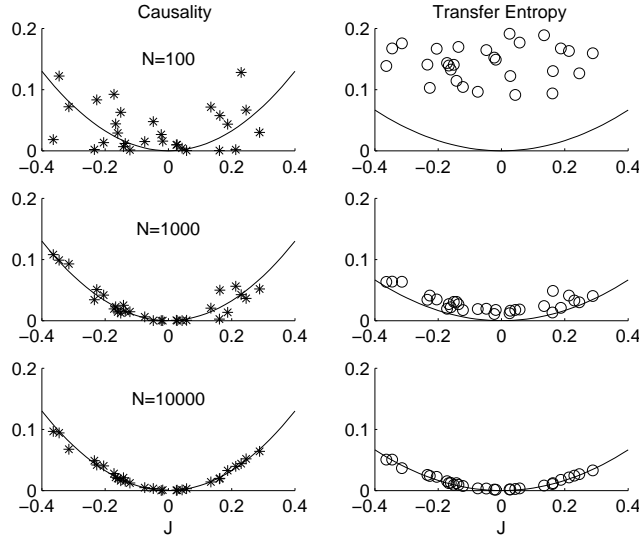


FIG. 2: For a typical asymmetric Ising model of six spins and $J_0 = 0.2$, the linear Granger causality (right) and the transfer entropy (left) are depicted for each link, as a function of its coupling J , for $N = 100$ (top), 1000 (middle) and 10000 (bottom) samples. The continuous curves represent the *true* values (obtained by fitting the points in fig. 1).

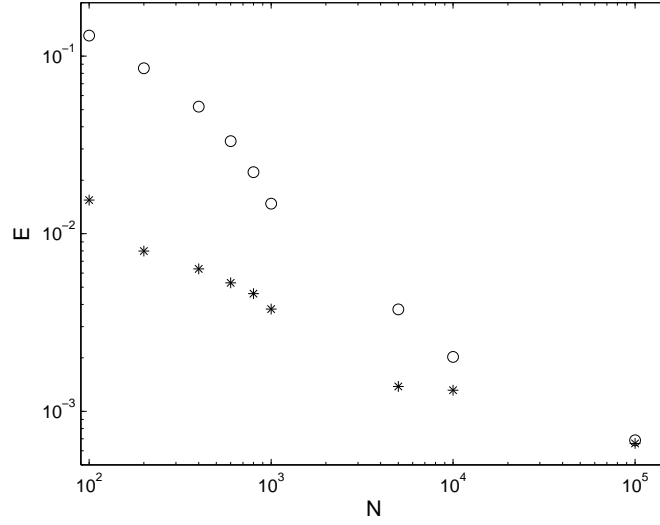


FIG. 3: The asymmetric Ising model described in figure 2 is here considered. Calling t_a the true value of the transfer entropy and t_b its estimate based on N samples, averaged over 1000 runs of the Ising system, we define $E = |t_b - t_a|/t_a$. The quantity E , thus obtained, is here plotted versus N (empty circles). A similar quantity E , concerning Granger causality, is also plotted (stars).

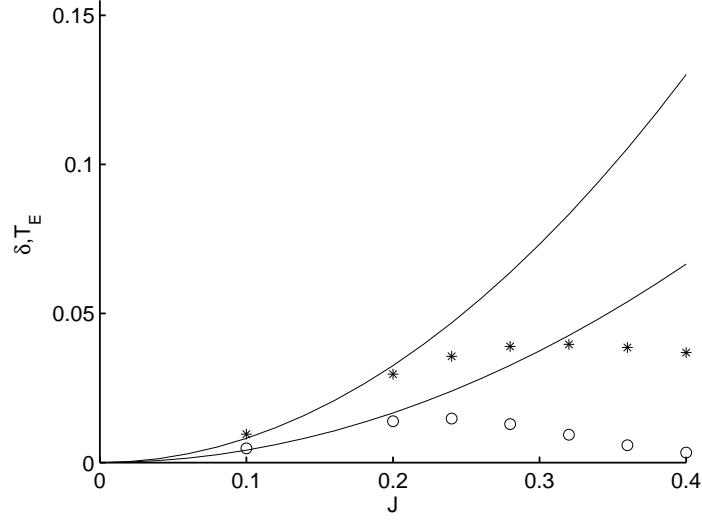


FIG. 4: The homogeneous Ising model, with $n = 6$ and uniform couplings $J > 0$, is considered. As a function of J , the linear Granger causality (stars) and the transfer entropy (empty circles) are depicted versus J . Both quantities are the same for all links, due to symmetry. The two curves are the relations between the coupling and transfer entropy (and between coupling and causality) which hold for the asymmetric Ising model (obtained by fitting the points of fig. 1).

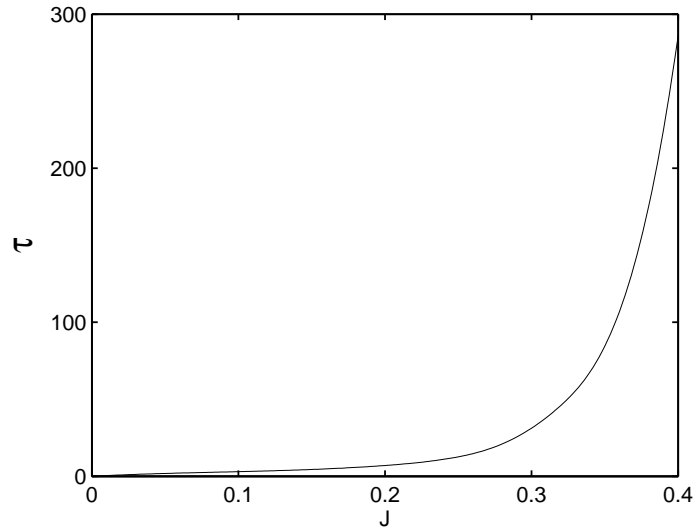


FIG. 5: The auto-correlation time of the magnetization for the homogeneous Ising model analyzed in figure 4.

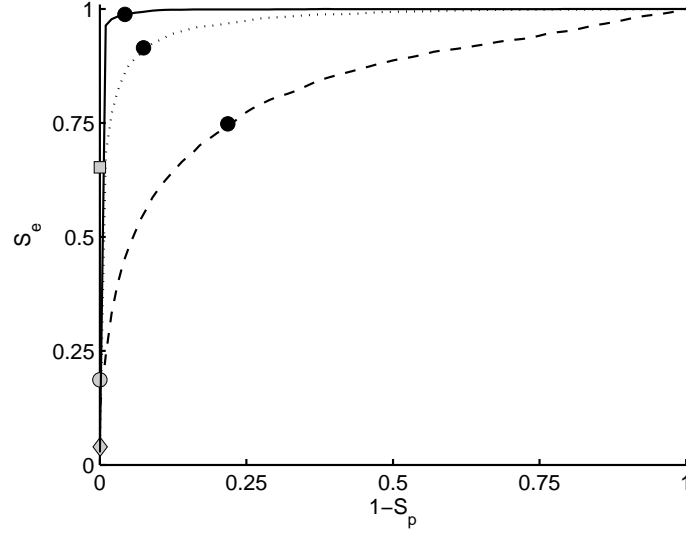


FIG. 6: The ROC curves (sensitivity vs 1-specificity) for the detection of non-vanishing couplings in the sparse system of 30 spins described in the text; the curves correspond to three values of the number of samples N , 100 (dashed line), 250 (dotted line) and 500 (continuous line). The stars on these curves represent the points found by ten-fold cross validation. The other three symbols are the performances by Granger causality on $N = 100$ (empty diamond), $N = 250$ (empty circle), $N = 500$ (empty square).

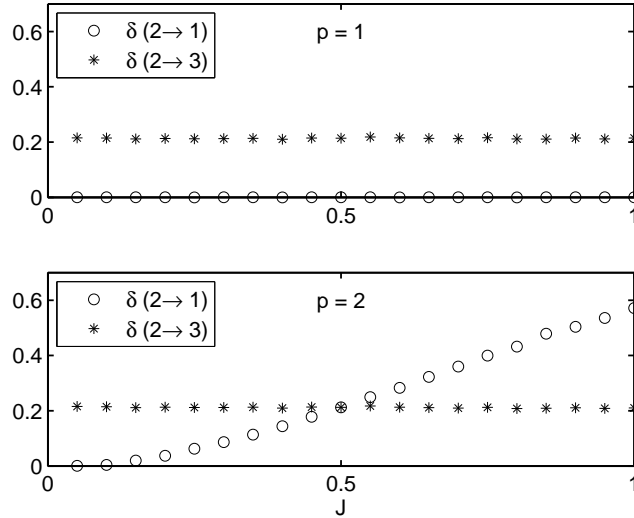


FIG. 7: The causalities $\delta(2 \rightarrow 1)$ and $\delta(2 \rightarrow 3)$ are depicted as a function of J for the three spins system described in the text. Causalities are estimated using the linear kernel (top) and the $p = 2$ polynomial kernel (bottom).

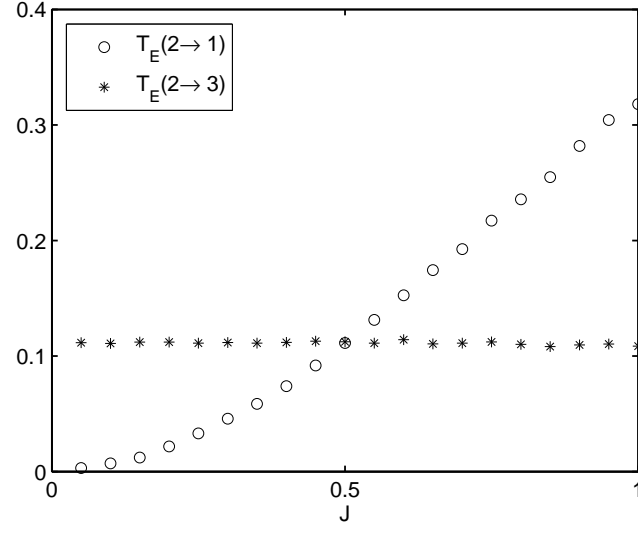


FIG. 8: The transfer entropies $T_E(2 \rightarrow 1)$ and $T_E(2 \rightarrow 3)$ are depicted as a function of J for the three spins system described in the text.